MAPPING OF DESERT BIOLOGICAL SOIL CRUST USING HYPERSPECTRAL WATER BANDS

Michael L. Whiting* and Susan L. Ustin

Center for Spatial Technologies and Remote Sensing
Department of Land, Air, and Water Resources, University of California, Davis, CA, USA
mwhiting@ucdavis.edu; slustin@ucdavis.edu

KEY WORDS: biological soil crust, soil moisture, water content, soil lichen, soil cyanobacteria

ABSTRACT:

Biological Soil Crust (BSC) species are important contributors to reducing erosion, and increasing soil organic matter and CO_2 exchange. Other investigators have demonstrated that respiration and photosynthesis are highly correlated to water content in soil lichen, such as *Collema* sp., and thus water content is one parameter in predicting CO_2 exchange. Our study of BSC cover consists of *Collema* sp. lichen and cyanobacteria on gravelly and sandy soil between shrubs, grass, and forbs common on hyperarid soils in the Mojave Desert in southwestern continental USA.

Laboratory and field spectral measurements of soil and BSC were used to predict measured surface water content and amount of crust. Linear regression of Soil Moisture Gaussian Model (SMGM), a SWIR spectral fitting function, was highly correlated to a sequence of water content in soil and BSC samples, $r^2 = 0.97$. When dry, SMGM combined with narrow-band water indexes predicted the BSC cover amount within the confidence intervals from field point-intercept measurements of cover (RMSE = 9.1 and 7.8 % cover, model and validation, respectively).

Spectra from pixels within a 5 November 2005 AVIRIS image at points of measured BSC cover content were used to generate a similar predictive model for cover with an (R^2 of 0.80 and RMSE = 4.2 % cover). After eliminating pixels of high NDVI values due to shrub cover, the model coefficients were used to create an AVIRIS BSC cover map.

This research leads the way to high resolution mapping of CO_2 exchange for carbon cycle models and identifying local disturbance of BSC regardless of soil and vascular plant backgrounds.

1. INTRODUCTION

Determining the amount of Biological Soil Crust (BSC) on the surface is essential to predicting the rate of CO_2 exchange contribution in arid environments. BSC is also a significant factor in reducing wind and rainfall erosion in areas lacking vascular vegetation. The loss of BSC is an indicator of desertification and degradation of the land surface. Models of global climate change are predicting an increase in moisture, and possibly nitric acids from urban pollution, in many arid regions. In these deserts, the impact of climatic change on the photosynthetic response by BSC will contribute substantially to variation in gas exchange. The activity of BSC was demonstrated to be a function of water content by Lange et al. (1998). Carbon dioxide exchange whether as photosynthesis or respiration was correlated to the water content in the gelatinous thallus of *Collema tenax* soil lichen. Burgheimer et al. (2006) was able to correlate the exchange of CO_2 to NDVI of BSC as indictor of activity.

*corresponding author

The CO_2 exchange is also a function of the amount of BSC surface area. Karnieli et al. (1999) spectrally separated BSC communities on sand dunes by light absorptions in the visible region by chlorophyll (670 nm), and in the infrared region by cellulose/lignin (1720 nm), starch/lignin/wax (2180 nm), humid acid/wax/starch (2350 nm) and water (1447, 1920 nm).

At our site, and in most of the US arid southwest, BSC grows on the open mineral soil surfaces between sparse shrubs. The rugose gelatinous lichen *Collema* sp. is generally found in gravel, particularly within gravel pavements. The cyanobacteria, such as *Microcoleus* sp. is commonly found in areas of wind sorted fine sands, and distinguishable by the pedestals formed by the gelatinous filaments within the soil that bind the mineral grains together and resist the erosive forces of rain.

These species were the dominant BSC and were commonly found growing together at our experiment site. The spectral indicators of BSC abundance determined by Karnieli et al. (1999) are not suitable due to NPV lignin and other organic matter, or using chlorophyll light absorptions during moist conditions when BSC are active since they are not separable from vascular plants. The remaining spectral regions available with strong absorptions are water bands, even during dry periods when imagery is generally acquired.

2. METHOD

2.1 Experiment Site

The Mojave Global Change Facility within the US Department of Energy Nevada Test Site (http://www.unlv.edu/Climate_Change_Research/MGCF/MGCF_index.html) is a long-term undisturbed ecological research site simulating the effects of increased precipitation during the summer monsoons (irrigation of 0 or 25 mm in each of three month) and nitrogen applications in late fall (0, 10, or 40 $kgha^{-1}$ annually) in 8 replicated treatments on square 14 m plots. In addition, the surfaces of half of these plots were trampled while the remaining plots were left undisturbed.

Some sparse shrubs remain green during the summer, such as Cresotebush (*Larrea tridentata*), while others lose their leaves and expose more branch bark, such as the mountain white burro bush (*Ambrosia dumosa*). Calcareous sandy soils formed on these hyperarid bajada slopes, often with a calcic horizon within 40 cm depth and/or a course gravel pavement (without varnish) surface. In other areas of the site the bajada surface has wind blown sand deposits (Titus et al. 2002). Though the study site is dissected by shallow channels, the plots were placed on uniform surfaces between the channels.

2.2 Spectral and cover data collections

This BSC study evaluated spectral data collected in three levels: endmember samples measured in the lab; ½ m diameter FOV measurements within field plots, and AVIRIS imagery of the entire site. Endmember field samples of soil, *Collema* sp., *Miconectous* sp., and short moss were mounted in shallow 15 cm Petri dishes and moistened with a bottle mister until thoroughly wet. Under full sun during July 2006 at UC Davis with daily temperatures approaching 40 °C and relative humidity below 40 %, weight and reflectance were measured every ½ h during the solar window for two days, and then on the fourth day for a fully dry measurement. The samples were stored when not being measured in low light and at ambient temperature. The lab data presented here are only the dry measurements.

The field plot spectral measurements were repeated in June, July, and August in 2005 and 2006 during the solar window before the irrigation treatments began.. A 1.2 m tall monopole with a 0.8 m extension held the optical cable tip of our ASD FieldPro spectrometer (ASD, Boulder, CO, USA) and a small digital camera. The cable tip and camera were held nadir using a bubble level mounted on the extension. Three measurements were made at azimuth SW, S, SE using a mounted compass, sweeping approximately 3 m. The monopod foot was located with DGPS. At selected samples, to reduce plot disturbance, point-intercept measurements were made of the spectrometer FOV using 5 cm increments on three rulers, approximately 121 points per 0.25 m^2 sample. The occurrence of the covers soil fine-fraction, gravel, NPV, photosynthetic vegetation, and BSC were tallied across the third ruler as it moved along the intervals of the other two rulers. Point-intercept measurements were made at 44 spectrometer sample points. Eleven of these measurements points were repeated by three or more observers to determine the variance within this cover measurement method.

The 5 November 2005 AVIRIS image was atmospherically corrected with ENVI-FLASH to approximate several ground invariant spectral measurements. The spectra were then empirically calibrated to these invariant targets. The image was geometrically corrected by the NASA, and a slight transform rotation adjustment was performed in ENVI to fit DGPS positions of access roads and RTK measured plot corners. The geometric accuracy was visually estimated at half to one pixel of the 3.2 m GSD.

2.3 Data processing

All spectra were preprocessed using IDL/ENVI (ITT Visual Solutions, Boulder, CO, USA) scripts by first eliminating bad-bands and smoothing with a Savitzky-Golay filter. Lab and field spectra were loaded to synthetic image cubes for analyzing both ASD and AVIRIS image spectra with the same IDL scripts. The lab and field spectra were analyzed by calculating a large number of narrow-band indexes. Abundance model parameters to apply to the AVIRIS image were determined using step-wise multiple regression and AIC in S-Plus statistical software (Insightful Corp. Seattle, WA, USA).

The combination of water indexes that gave the best prediction were Normalized Difference Water Index (NDWI, Gao, 1996), Water Band Index (WBI, Peñuelas et al. 1997) and Moisture Stress Index (MSI, Hunt and Rock, 1989). As well as one index that is less well known the Soil Moisture Gaussian Model (SMGM, Whiting et al. 2004). This technique fits an inverted Gaussian function to the log transformed spectra from the point of maximum reflectance to the fundamental water absorption at 2800 nm (beyond our instrument's limit). Whiting et al. (2004) found the area within the inverted Gaussian was highly predictive of the surface water content of soil.

3. RESULTS AND DISCUSSION

3.1 Determination of surface water content

The laboratory measurements of the soil and BSC endmembers were made through the drying sequence and were used to relate water content by weight to the area of the inverted SWIR Gaussian (SMGM). SMGM was strongly predictive of gravimetric water content for soil, *Collema*, cyanobacteria, and moss endmembers, together and individually. In Figure 1, the SMGM separates the moisture content of each endmembers while the gravimetric water content includes the soil water below the optical thickness of the surface.

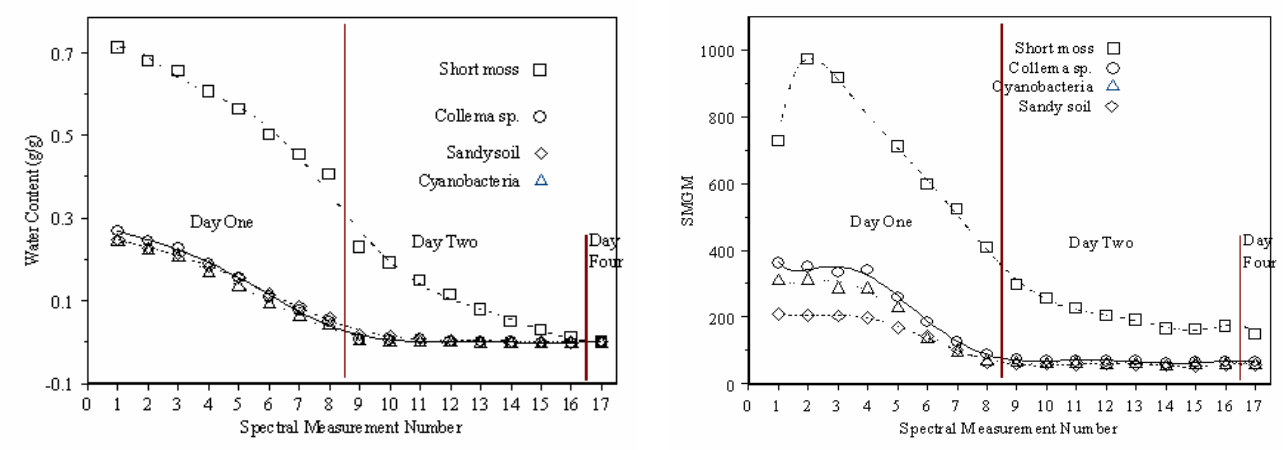

Figure 1. Comparison of a) gravimetric water content and b) SMGM water index over several days of spectral measurements.

3.2 Determining BSC surface area

The cube of lab spectra was a synthetic linear mixture of each endmember spectra of BSC (as ½ *Collema* and ½ cyanobacteria spectra), soil, and gravel in 5 % increments at each moisture level. The gravel endmember was a field spectral measurement of pure dry pavement. The vegetative narrow-band indexes, individual or in multiple combinations, were poor or not predictive of the proportion of BSC in the mixture. Several combinations of water indexes were significantly correlated to the synthetic mixture. For example, SMGM, WBI, NDWI returned a R^2 of 0.99, and standard error of 0.0085 (0.85 % BSC cover) for the 230 mixed spectra.

With ASD ground measurements, the combination of SMGM, WBI and MSI was, in this case, slightly better with an R^2 of 0.88 and standard error of 0.070 (7.0 %) for 44 field spectra where there was at least one point-intercept measurement. The range in the amount of measured BSC cover was 0 % to 56 %. Applying the model from the lab synthetic mixture provides some indication of the robustness of this technique, where the R^2 was 0.52, although this model generally over estimated the amount of BSC cover. The variance from the repeated point-intercept measurements was used to calculate the confidence limits in Figure 2. The predictions of BSC cover using the field spectral model was generally within these limits.

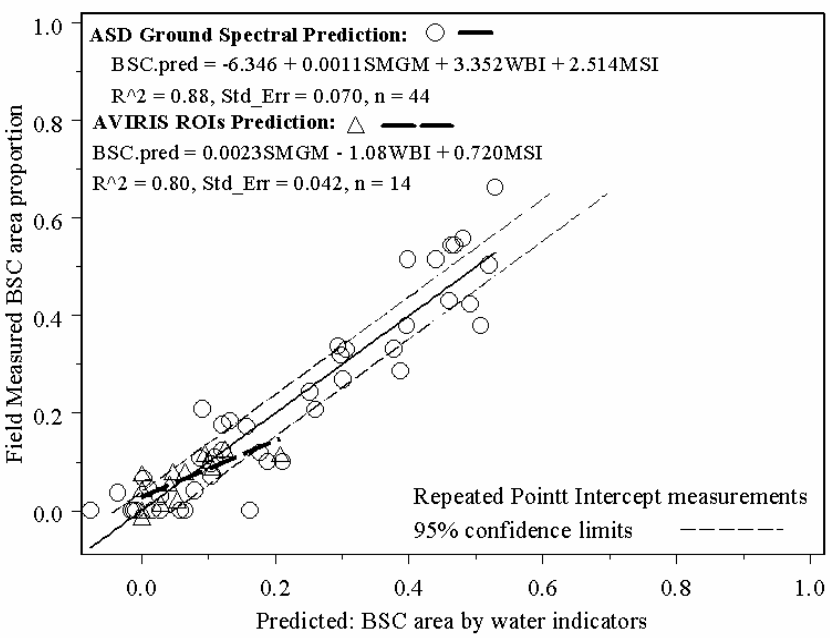

Figure 2. AVIRIS model compared to ASD ground measurements in prediction amount of BSC cover.

The water indexes were used to generate a prediction model of BSC cover for the entire study site by carefully georectify and

extracting individual pixel spectra from the AVIRIS image at field measured pixels (Figure 2). We assumed the three ASD measurements (0.6 m^2) in a sweep through a pixel area (10.2 m^2) is an adequate sample. The mean of the point-intercept measurements within the pixel diminished the range in BSC cover to 0 % to 16 %. In Figure 2, the predictive model using AVIRIS spectra is within the confidence limits, but has lower trajectory due to the fewer number of measurements (14) and the narrow range in BSC cover. The R^2 remained high (0.80), and the standard error improved significantly to 0.042 (4.2 % cover).

3.3 Mapping BSC surface area

The AVIRIS was processed by eliminating pixels of green vegetation and ultra bright soil of the roads and other bare areas by creating a processing mask between -0.03 and 0.15 NDVI. These values were chosen by inspection. The pixel predictive model was applied to the masked regions within the AVIRIS image shown in Figure 3 a). The image was classified using K-means, which resulted in intervals that approximated the standard error in Figure 3 b). Approximately 32 % of the image was outside the mask. The edges of the roads, eroded drains, and disturbed areas where there no BSC occur are shown in red. Moderate and high amounts of BSC are dispersed throughout the image. Notable is the high concentration of BSC cover seen in yellow and cyan in the gravel beds

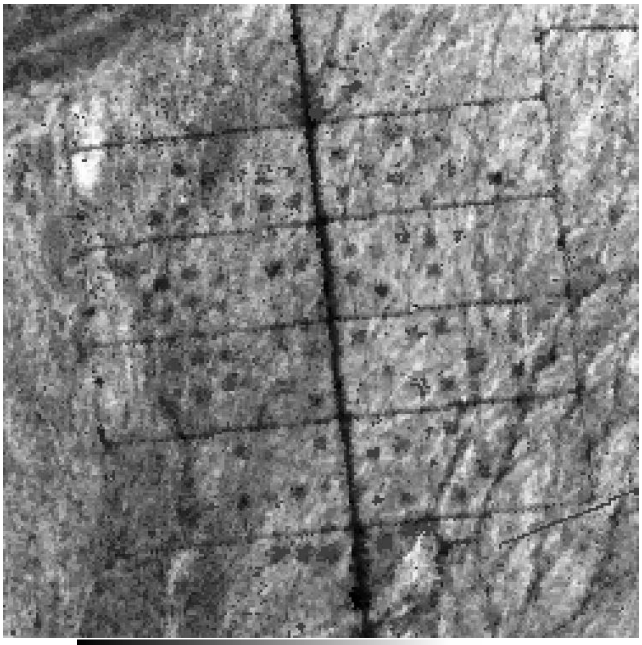

a)

Unclassified 0.16+

b)

Class	Color	Area
Unclassified	(black)	32.4%
-0.03 – 0.02	(red)	11.2%
0.03 – 0.05	(green)	13.6%
0.06 – 0.08	(blue)	17.2%
0.09 – 0.11	(yellow)	17.0%
0.13 – 0.16+	(cyan)	7.1%

Fig. 3 a) Gray-scale of estimated BSC cover from AVIRIS image, and b) K-means classification of cover.

that can be seen from the access roads in NW and SE corners of the image. The pattern of the cyan class is similar to the location of the loess deposits in the NE quadrant were cyanobacteria is abundant.

4. CONCLUSIONS

This research has demonstrated that spectrally detected differences in water content between BSC and bare soil can be used to determine the amount of BSC cover. The regions of high light absorption by water at 970, 1140, 1410, and 2800 nm were exploited for these prediction models. These spectral measurements were made on dry sandy and gravelly surfaces that were mixed with BSC and NPV, with no gravimetrically detectable water content within 0.01 %. The natural desert surfaces were measured after several weeks of extreme surface temperatures and low humidity. The high radiometric and spectral resolution necessary to quantify the water absorptions were made with ASD field spectrometer and AVIRIS imaging spectrometer.

REFERENCES

Burgheimer, J., B. Wilske, K. Maseyk, A. Karnieli, E. Zaady, D. Yakir, and J. Kesselmeier, 2006. Ground and space spectral measurements for assessing the semi-arid ecosystem phenology related to CO2 fluxes of biological soil crusts. *Remote Sensing of Environment* 101:1-12.

Gao, B., 1996. NDWI--A normalized difference water index for remote sensing of vegetation liquid water from space. *Remote Sensing of Environment* 58:257-266.

Hunt, E.R., Jr., and B.N. Rock, 1989. Detection of changes in leaf water content using near- and middle-infrared reflectance. *Remote Sensing of Environment* 30:43-54.

Karnieli, A., G.J. Kidron, C. Glaesser, and E. Ben-Dor, 1999. Spectral characteristics of cyanobacteria soil crust in semiarid environments. *Remote Sensing of Environment* 69:67-75.

Lange, O.L., J. Belnap, and H. Reichenberger, 1998. Photosynthesis of the cyanobacterial soil-crust lichen *Collema tenax* from arid lands in southern Utah, USA: role of water content on light and temperature responses of CO_2 exchange. *Functional Ecology* 12:195-202.

Peñuelas, J., J. Piñol, R. Ogaya, and I. Filella, 1997. Estimation of plant water concentration by the reflectance Water Index (R900/ R970). *International Journal of Remote Sensing* 18:2869-2875.

Titus, J.H., R.S. Nowakw, and S.D. Smith, 2002. Soil resource heterogeneity in the Mojave Desert. *Journal of Arid Environments* 52:269–292.

Whiting, M.L., L. Li, and S.L. Ustin, 2004. Predicting water content using Gaussian model on soil spectra. *Remote Sensing of Environment* 89:535-552.

ACKNOWLEGEMENTS

We thank Lynn Fenstermaker, Director, and MGCF Staff for access and support of the field trials. This research was supported by the Office of Science, Biological and Environmental Research Program (BER), U.S. Department of Energy, through the Western Regional Center of the National Institute for Global Environmental Change (NIGEC) under Cooperative Agreement No. DE-FCO2-03ER63613. Financial support does not constitute an endorsement by DOE of the views expressed in this report.